

INNOVATIVE BOLTED BEAM-TO-COLUMN JOINTS IN MOMENT RESISTANT BUILDING FRAME: FROM EXPERIMENTAL TESTS TO DESIGN GUIDELINES

Hoang Van-Long, Demonceau Jean-François, Jaspart Jean-Pierre
ArGEnCo Department, University of Liège, Belgium
s.hoangvanlong@ulg.ac.be; jfdemonceau@ulg.ac.be; jean-pierre.jaspart@ulg.ac.be

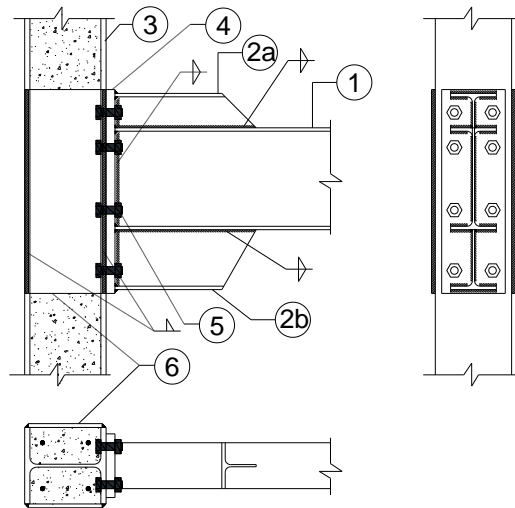
1. INTRODUCTION

Within the framework of the RFCS European project HSS-SERF – “High Strength Steel Seismic Resistant Building Frames”, a work package (WP 4) was devoted to the investigation of innovative bolted beam-to-column joints in moment-resisting dual-steel frames susceptible to be loaded by significant seismic actions. Respecting the capacity design approach, the structural joints should be full strength ones, taking into account the possible overstrength as recommended in Eurocode 8. One of the specificities of the HSS-SERF project was that the proposed joints were intended to be used in moment resistant dual-steel frames where the beams are made of S355 steel grade while S460 or S700 steel grades are used for the steel profiles/tubes in the composite columns.

Three bolted end-plate joint configurations were proposed: (1) Bolted hammer head end-plate to wide flange column joint (B-EP-H) (Figure 1): the end-plate welded to the hammer head beam is directly bolted to the flanges of partially-encased wide-flange columns reinforced by lateral plates (pieces 6 in Figure 1); (2) Bolted hammer head end-plate to RHS column joint with U channel (B-EP-U) (Figure 2): the end-plate welded to the hammer head beam is connected to a concrete-filled tube column through a reverse U channel (pieces 6 in Figure 2); and (3) Bolted extended end-plate to RHS column joint with long bolts and reduced beam section (B-EPL-RBS) (Figure 3): extended end-plates are bolted to concrete-filled tube column using long bolts passing through the column.

Through a preliminary analysis, it has been identified that the following points require new developments because they are not covered yet by the Eurocodes and, in particular, by EN1993-1.8 devoted to joints.

- Characterisation of the compression zone and of the lever arm of the B-EP-H and B-EP-U joints (using hammer head beams).
- Characterization of the hammer head component in compression/tension for B-EP-H and B-EP-U joints.
- Characterization of the column flange in bending component (with lateral plates) in B-EP-H joints.
- Characterization of the reverse U channel component in B-EP-U joints.
- Consideration of the preloading of the long bolts in the prediction of the stiffness of the B-EPL-RBS joints.
- Determination of the resistance of the beam in the hammer head zone for the B-EP-H and B-EP-U joints.



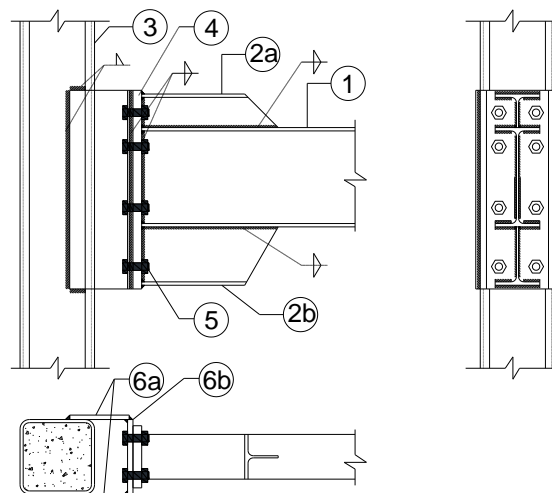
Elements

- 1 Double-T steel beam
- 2a, 2b Top and bottom hammer- heads
- 3 Partially-encased wide-flange column
- 4 End-plate
- 5 Bolts
- 6 Lateral plates

Steel materials

- S355
- Extracted from the beam profiles
- S460 / S700
- S355
- 10.9
- Same grade with the column profiles

Figure 1: B-EP-H joint configuration



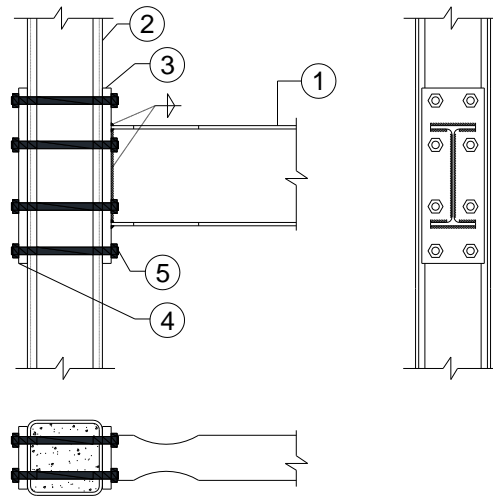
Elements

- 1 Double-T steel beam
- 2a, 2b Top and bottom hammer-heads
- 3 Concrete-filled RHS column
- 4 End-plate
- 5 Bolts
- 6a, 6b Lateral faces and front face of U channel

Steel materials

- S355
- Extracted from the beam profile
- S460 / S700
- S355
- 10.9
- Same grade with column tube

Figure 2: B-EP-U joint configuration



<i>Elements</i>		<i>Material</i>
1	Double-T steel beam with dog-bone	S355
2	Concrete-filled RHS column	S460 / S700
3	End-plate	The same grade with the beam
4	Repartition plate	The same grade with the beam
5	Long bolts	10.9

Figure 3: B-EPL-RBS joint configuration

In order to validate these required developments through experimental evidences, a test campaign was defined and performed at the University of Liège, a project partner (Section 2). In parallel, analytical developments have been carried out to propose new design rules for components not yet covered by the Eurocodes with the final aim of allowing a complete analytical characterisation of the proposed innovative joints (Section 3). In Section 4, the validation of the developed models through a comparison with the experimental results is presented.

2. EXPERIMENTAL TESTS

16 large scale specimens were tested within the test campaign (Table 1): 8 B-EP-H joints, 4 B-EP-U joints, and 4 B-EPL-RBS joints. The test specimens were extracted from reference buildings designed within work package 1 of the HSS-SERF project. HEB320/260 profiles and 300x10/250x10 square hollow sections are used for the columns made of S460/S700 steels while IPE400 with S355 steel grade is used for the beams in all specimens. As the joints have been designed to be full strength, the beams in some specimens are reinforced by welding vertical plates between the flanges (see Figure 7) to be able to reach the resistance of the joints during the tests and, so, to characterise the behaviour of the previously identified new components.

The test set-up for the beam-to-column joints is presented in Figure 8. Fixed hinges at the bottom and hinges allowing a vertical displacement at the top are used at the column extremities. Possible displacements of the hinges have been anyway recorded during the tests. A vertical load is applied at the free end of the beam introducing a bending moment and a shear force in the joints.

Table 1: description of the tested specimens

N ^o	Test	Joint type	Column	Detail	Reinforcement degree (Figure 7)	Loading ^(a)
1	A1	B-EP-H	HEB 320, S460	Figure 4	partially reinforced	Monotonic M ⁺
2	A2				totally reinforced	Monotonic M ⁻
3	A3				not reinforced	Monotonic M ⁺
4	A4				not reinforced	Cyclic
5	B1		“HEB260”, S690		totally reinforced	Monotonic M ⁺
6	B2				totally reinforced	Monotonic M ⁻
7	B3				not reinforced	Monotonic M ⁺
8	B4				not reinforced	Cyclic
9	C1	B-EPL-RBS	SHS 300x300x12.5, S460	Figure 4	totally reinforced	Monotonic M ⁺
10	C2			totally reinforced	Monotonic M ⁻	
11	D1	B-EP-U		Figure 4	not reinforced	Monotonic
12	D2			Figure 6	not reinforced	Cyclic
13	E1	B-EPL-RBS	SHS 250x250x10 S700	Figure 4	totally reinforced	Monotonic M ⁺
14	E2			Figure 5	totally reinforced	Monotonic M ⁻
15	F1	B-EP-U		Figure 4	not reinforced	Monotonic
16	F2			Figure 6	not reinforced	Cyclic

^(a): M⁺ and M⁻ are hogging and sagging moments, respectively; ANSI/AISC 314-10 protocol is used in the cyclic tests.

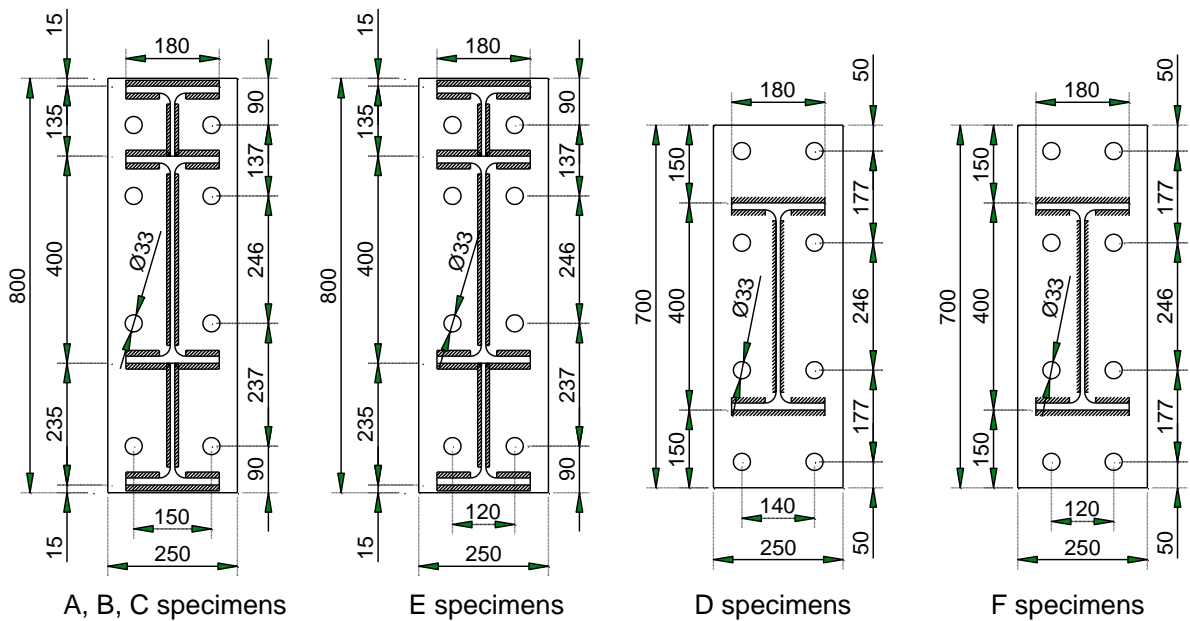


Figure 4: end-plate details

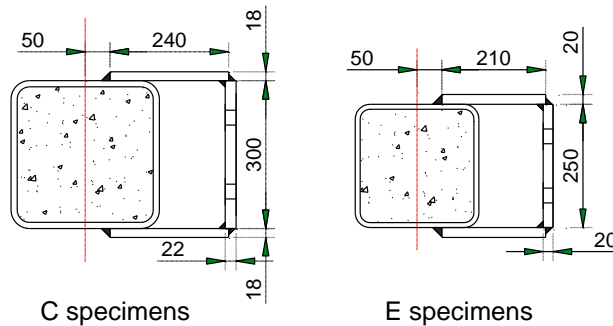


Figure 5: reverse U channel details

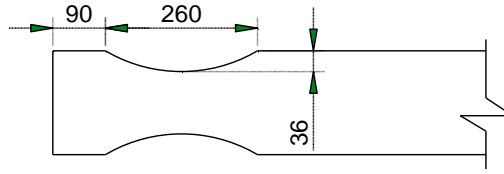


Figure 6: dog-bone detail (D and F specimens)

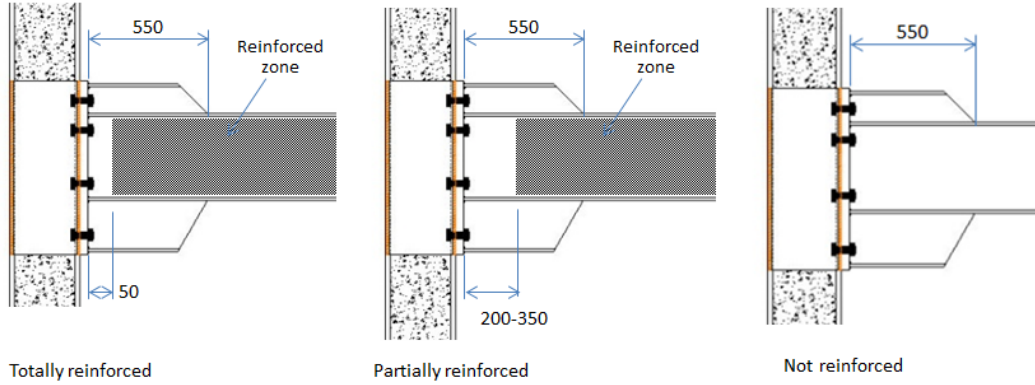


Figure 7: different reinforcements of the beams

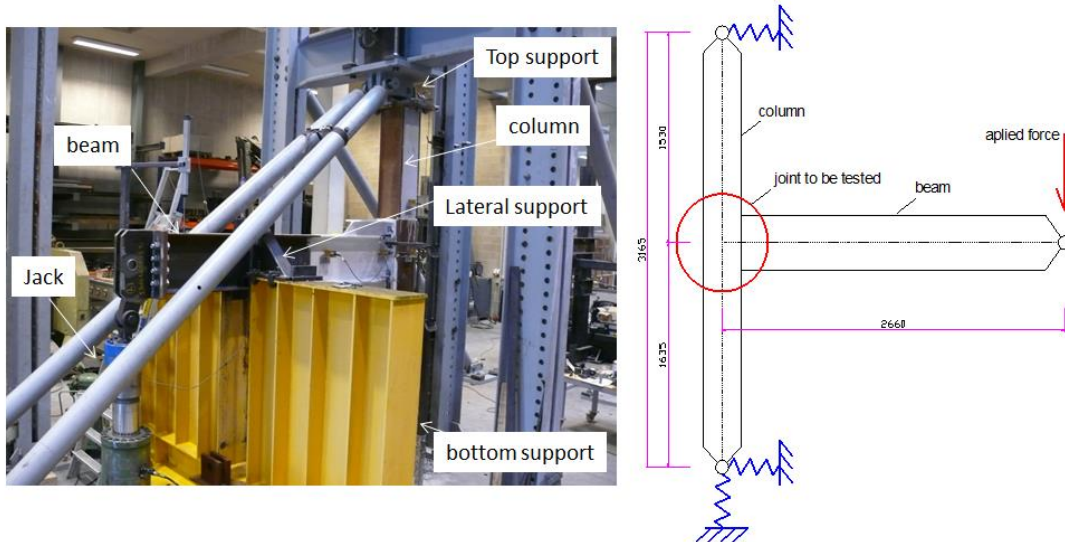


Figure 8: Test set-up

The main test results (i.e. the resistance, the initial stiffness and the failure modes) are presented in Table 2. Additional information such as the coupon tests for the material characterisation, the geometric measurement, the instrumentation, the bolt tightening, etc. can be found in the deliverable report D4 of the present project available on request to the authors.

The average stiffness of each joint type is shown in Figure 12 through the k_b factor representing the relative stiffness between the joint ($S_{j,ini}$) and the associated beam (EI_b/L_b). The moment rotation curves are not reported herein by the detailed curves recorded during the tests can be found in Deliverable D4 of the presented project. The following remarks can be drawn from the test results: (1) all the joints are full strength ones; (2) B-EP-H and B-EPL-RBS have a high stiffness while the stiffness of the B-EP-U joint decrease due to the deformability of the reverse U channel; (3) different failure modes have been observed allowing validating the developments related to the new joint components.

Table 2: test results

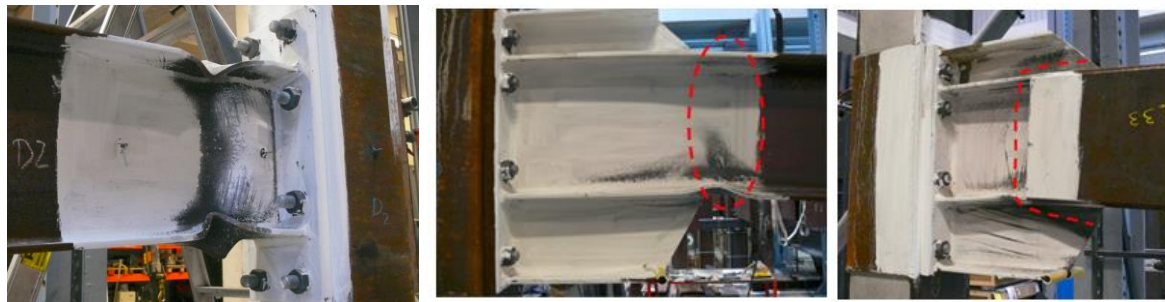
Test	$M_{\max}^{(a)}$ (kNm)	Stiffness ^(b) (kNm/rad)	Failure modes
A1	820	193 000	Plastic hinge in the hammer head zone (Figure 9)
A2	1187	187 000	Joint failure (bolts + hammer head) (Figure 10)
A3	550	210 100	Plastic hinge in the beam (Figure 9)
A4	575	182 400	Plastic hinge in the beam (Figure 9)
B1	1160	154 500	Joint failure (bolts + hammer head) (Figure 10)
B2 ^(c)	944	177 700	
B3	550	214 000	Plastic hinge in the beam (Figure 9)
B4	566	144 000	Plastic hinge in the beam (Figure 9)
C1	980	82 027	Yield mechanic in reverse U channel (Figure 11)
C2	877	80 000	Yield mechanic in reverse U channel (Figure 11)
D1	435	154 900	Plastic hinge at the dog-bone (Figure 9)
D2	437	144 820	Plastic hinge at the dog-bone (Figure 9)
E1	972	70 100	Yield mechanic in reverse U channel (Figure 11)
E2	946	68 300	Yield mechanic in reverse U channel (Figure 11)
F1	435	113 850	Plastic hinge at the dog-bone (Figure 9)
F2	433	112 950	Plastic hinge at the dog-bone (Figure 9)

Remarks:

(a): maximal bending moment at the critical section.

(b): in the cyclic tests, the stiffness under hogging moment is reported.

(c): the weld between the beam and the reinforcing plate failed and the test was stopped.



At dog-bone

in the beam close to the hammer heads

in the hammer head zone

Figure 9: plastic-hinge failure mode

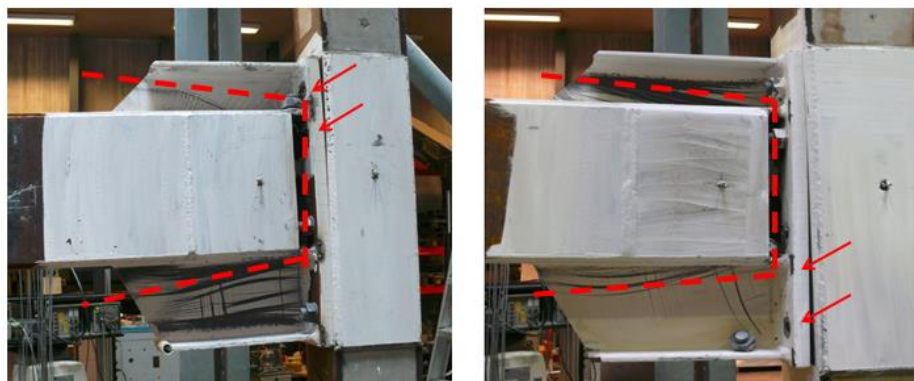


Figure 10: B-EP-H joint – failure in the connection
(4 bolts in the tension zone failed and the hammer head in compression yielded)

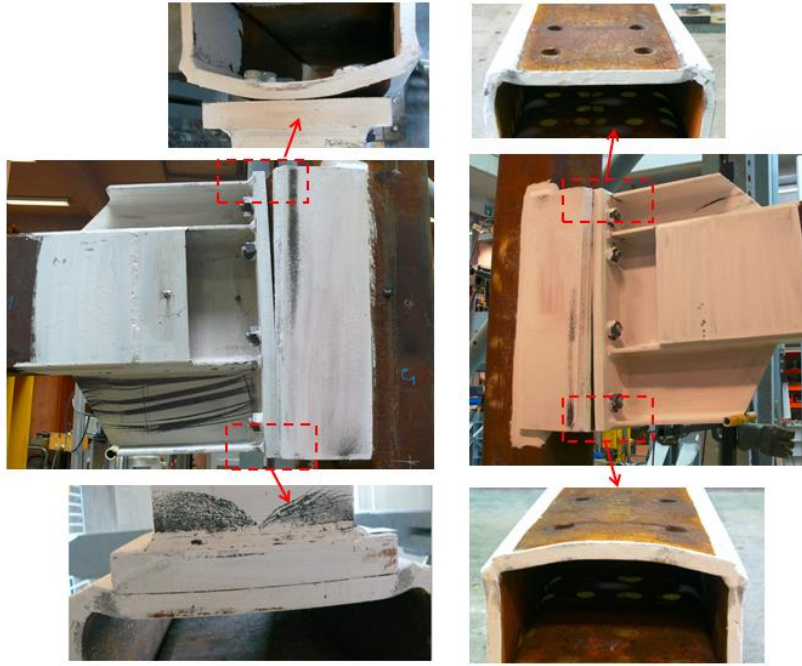


Figure 11: failure mode of the B-EP-H joints (reverse U channels yielded)

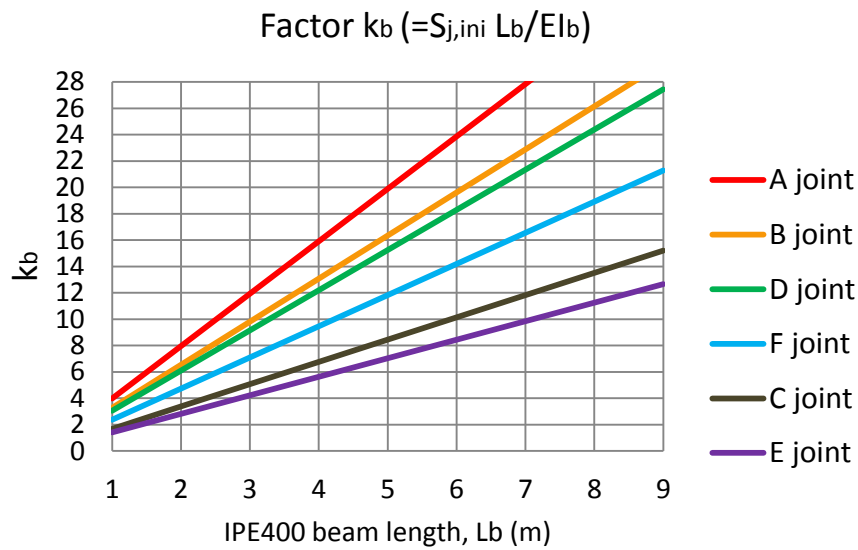


Figure 12: k_b factor for the joint types

3. DESIGN GUIDELINES

The component method is recommended in EN1993-1.8 for the design of structural joints; Table 1 presents the different components met in the investigated joints and references to Eurocode design rules when available. The new components not yet covered are also identified and reference is made to the section of the present paper where they are investigated. Some specific considerations about the application of the over-strength factor as recommended in EN1998-1.1 have been also addressed within the HSS-SERF project and can be found in Comelgau et al (2012b); these considerations are not repeated herein.

Table 3: identified joint components and available design rules

Individual component					Design rules
N°	Components	concerned joint types			
		B-EP-H	B-EP-U	B-EPL-RBS	
1	Column panel in shear	x	x	x	Covered in EN-1993-1.8 and EN-1994-1.1.
2	Column in transverse compression	x		x	
3	Beam web in tension	x	x	x	
4	Bolt in tension	x	x	x	
5	End-plate in bending	x	x	x	
6	Column web in tension	x			
7	Beam flange and web in compression	x	x	x	
8	Column flange in bending	x			Section 3.4
9	Hammer head in compression/tension	x	x		Section 3.2
10	U channel in bending		x		Section 3.3
11	Resistance of beam in the hammer head zone	x	x		Section 3.6
Component assembly					
1	B-EP-H and B-EP-U joints				Section 3.1
2	B-EPL-RBS joints				Section 3.5

3.1. Component assembly for B-EP-H and B-EP-U joints

The assembly rule given in EN-1993-1.8 can be applied for the investigated joints but a specificity in the compression zone needs to be considered.

Usually, a unique compression zone is considered for a joint; the stresses in the compression zone are assumed to be uniformly distributed in the beam flange. In the joints using hammer heads, two compression zones may be identified: one located at the hammer head flange and one at the beam flange. However, an equal distribution of the stresses between the two zones is not correct and a specific distribution between the hammer head flange (zone 1) to the beam flange (zone 2) (Figure 13) should be considered. It is proposed to estimate the compression force distribution between the two zones through the following equations.

$$\left[\begin{array}{l} F_{zone1} = \min(F_{Rd,zone1}; F_{Rd,row1} + F_{Rd,row2}) \quad \text{for B-EP-H joint} \\ F_{zone1} = \min(F_{Rd,zone1}; F_{U,zone1}) \quad \text{for B-EP-U joint} \end{array} \right. \quad (1)$$

$$F_{zone2} = \min(F_{Rd,zone2}; F_{Rd,row1} + F_{Rd,row2} - F_{zone1}) \quad (2)$$

In Eqs.(1) and (2), F_{zone1} and F_{zone2} are the compression forces developing in the zones 1 and 2 respectively. $F_{Rd,zone1}$ and $F_{Rd,zone2}$ are the resistances of the governing components in zones 1 and 2, respectively; $F_{Rd,row1}$ and $F_{Rd,row2}$ are the design resistances of bolt rows 1 and 2 in tension, respectively; $F_{U,zone1}$ is the compression force in the zone 1 concerning the U channel component, this quantity will be detailed in Section 3.3.

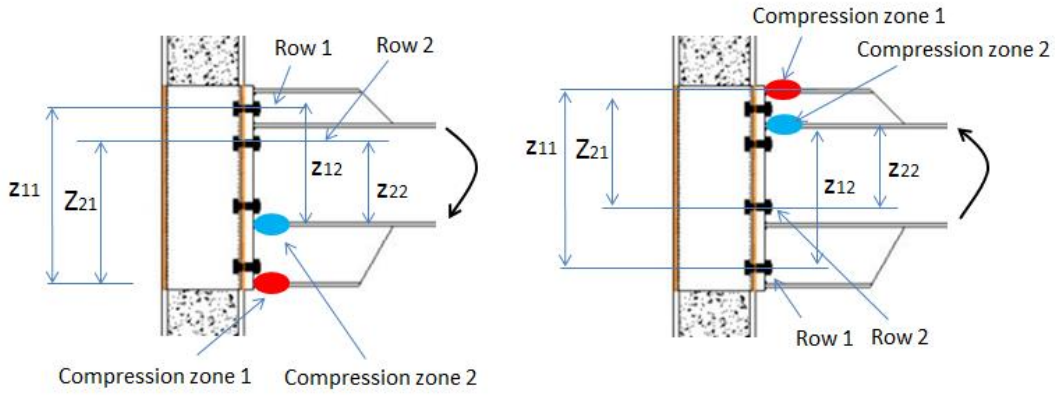


Figure 13: Definition of the compression zones

Above rule is applied for estimating the joint resistance, while only the compression zone 1 should be used for calculating the stiffness as, in the elastic domain, only this zone is assumed to be activated.

3.2. Hammer-heads in compression/tension component

Three mechanisms shown in Figure 14 should be considered for the “hammer head in compression/tension” component. The shear mechanism is considered for the hammer heads in both compression and tension zones while the compression and tension mechanisms are respectively adopted for the hammer heads in the compression or tension zone. The characterisation of the “haunched beam” and “beam web in tension” components is covered by EN-1998-1.8; these rules can be easily adapted to the compression and tension mechanisms respectively met within the present joint configuration. The resistance of the shear mechanism is taken as equal to the resistance in shear of the hammer head web added to the resistance of the end-plate and hammer head flange in bending (see Figure 14) at the image of what is done for a column web panel in shear stiffened by transverse horizontal plates. However, in most of the cases, the contribution of the hammer head web in shear is preponderant and therefore the contribution of hinges forming in the end-plate and the hammer head flange may be neglected. The resistance of the shear mechanism can be formulated as:

$$F_{Rd,hammer-head,shear} = l_h t_w f_{yb} / \sqrt{3} \quad (3)$$

with l_h is the length of the hammer head web (Figure 14); t_w is the thickness of the hammer head web; f_{yb} is the yield strength of the hammer heads.

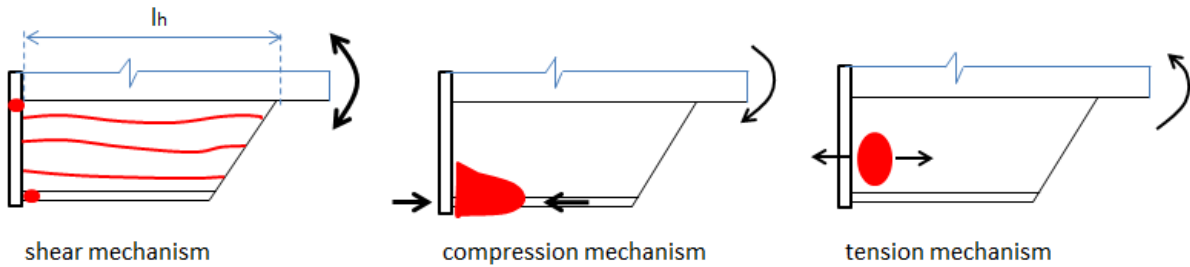


Figure 14: considered mechanisms for the hammer head component

3.3. Reverse U channel component

- *Tension zone behaviour*

Normally, the group effect is the critical one for the bolt rows 1 and 2. Two plastic mechanics (Figure 15), non-circular pattern and circular pattern, are considered, the smallest value is used for the determination of the component resistance. Due to the high tension force in the lateral faces, a linear interaction between the moment and axial force appearing in the plastic line developing in the lateral plates is taken into account. Finally, the distribution of the forces in the bolt rows 1 and 2 may be respectively determined by the following equations:

$$F_{U,row1} \leq \min \left[\frac{2m_{p,f}}{1 + \frac{t_l}{2(b-c)}} \left(\frac{2(\eta+1)e_1}{b-c} + 2\sqrt{\eta+1} \sqrt{\frac{2b}{b-c}} \right); 2m_{p,f} \left(\frac{2e_1}{r} + \frac{c}{r} + \pi \right) / \left(1 + \frac{t_l}{4r} \right) \right] \quad (4)$$

$$F_{U,row2} \leq \min \left[\frac{2m_{p,f}}{1 + \frac{t_l}{2(b-c)}} \left(\frac{2(\eta+1)e_2}{b-c} + 2\sqrt{\eta+1} \sqrt{\frac{2b}{b-c}} \right); 2m_{p,f} \left(\frac{2e_2}{r} + \frac{c}{r} + \pi \right) / \left(1 + \frac{t_l}{4r} \right) \right] - F_{Rd,row1} \quad (5)$$

where: $m_{p,f}$ is the resistant plastic moment per unit length of the U front face; η is the ratio between the resistant plastic moment per unit length of the U front face and U lateral face; t_l is the thickness of the U lateral face; e_1 , b , c and r are shown in Figure 15; $F_{Rd,row1}$ is the design resistance of the critical of the bolt row 1.

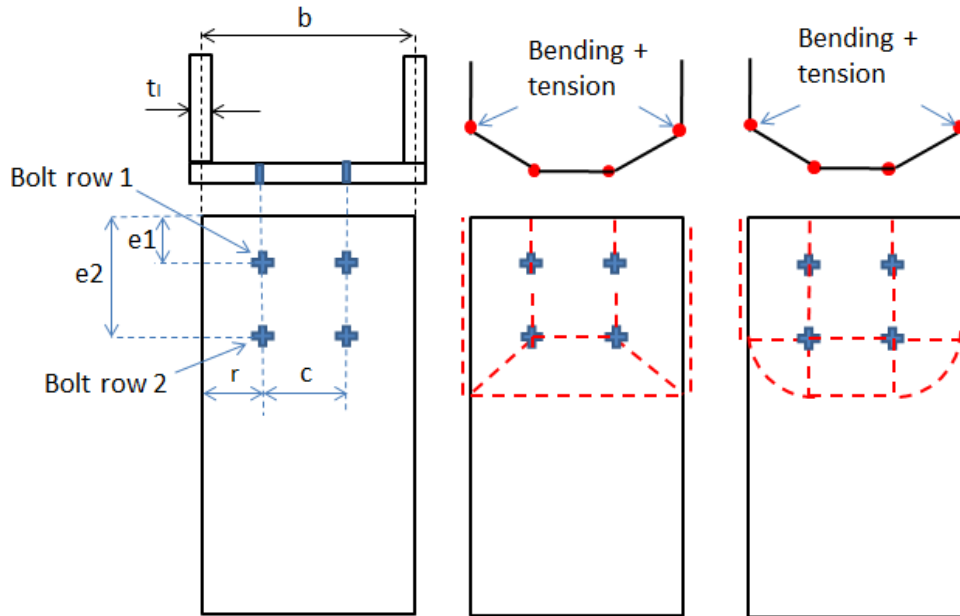


Figure 15: considered mechanisms for the U channel in tension

- *Compression zone behaviour*

Due to the contact effect of the end-plate, the resistance of the compression zone is always greater than the resistance of the tension zone, meaning that the U channel in compression is not the critical zone. Therefore, the important is not the resistance of the U channel in the compression zone, but the force distribution in the

compression zones 1 and 2 (Figure 13) needed to be determined. The global mechanism is considered for the U channel face in the compression zone (Figure 16), the increase of the load leads to the increase of the width of the compression zone (x in Figure 16). The bending or shear mechanisms may develop depending on the end-plate width in comparison with the U front face one. Two these mechanisms should be examined and the smallest value is applied. The distribution of the compression force in zone 1 and 2 can be determined by the following equation.

$$F_{U,zone1} \leq \left[m_{p,f} \left(\frac{8x^2x_1(1+\eta)}{8m(x_1^2+x_2^2)+x(x_1+x_2)t_l} + \frac{b_p x_1}{x(x_1+x_2)} \right), \frac{x^2 x_1 f_{y,f} t_f}{\sqrt{3}(x_1^2+x_2^2)} \right] \quad (6)$$

$$F_{U,zone2} = F_{Rd,row1} + F_{Rd,row2} - F_{U,zone1} \quad (7)$$

with $m_{p,f}$, η and t_l defined in Eqs. (3) and (4); b_p , the end-plate width; $f_{y,f}$, the yield strength of the U front face; x , the height of the compression part; $F_{Rd,row1}$ and $F_{Rd,row2}$ are the critical values of the resistance of the bolt rows 1 and 2, respectively, in the tension zone; x_1 and x_2 , respectively the distances from the hammer head flange centre and beam flange centre to the extremity of the compression zone as represented in Figure 16.

For a given joint configuration, x_1 and x_2 can be expressed as functions of x while the latter may be obtained from the equilibrium between the tension and the compression forces:

$$\min \left[m_{p,f} \left(\frac{8x^2(x_1+x_2)(1+\eta)}{8m(x_1^2+x_2^2)+x(x_1+x_2)t_l} + \frac{b_p}{x} \right), \frac{x^2(x_1+x_2)f_{y,f}t_f}{\sqrt{3}(x_1^2+x_2^2)} \right] = F_{Rd,row1} + F_{Rd,row2} \quad (8)$$

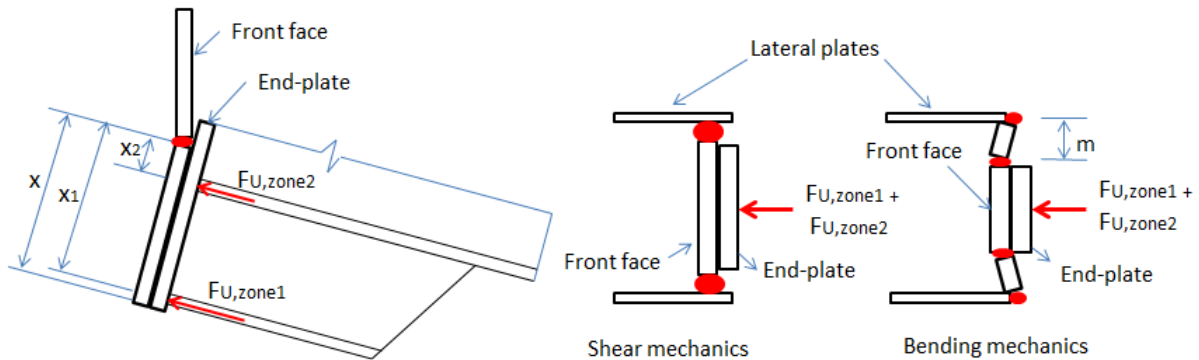


Figure 16: considered mechanisms for the U channel under compression

Remarks: above rules are used for estimating the joint resistance, the formulas take into account both front and lateral faces contributions. In the calculation of the initial stiffness, the formulas given in Lui (2012) can be used for the front face contribution while the “H-profile column web” component covered in EN-1993-1.8 can be applied to computer the contribution of the lateral faces.

3.4. Column flange in bending (in B-EP-H joint)

The column cross section made of a H-profile and lateral plates as illustrated in Figure 17 is equivalent to two hollow sections next to each other. Accordingly, this component may be seen as a face of a rectangular hollow cross section in

transverse tension, with only one bolt on one horizontal row. In literature, such component is not explicitly covered. However, many works have been developed the “column face”/or “column web” in bending as given in Figure 17 (e.g. Mágala-Chuquitaype (2010b) and Jaspart (2005)); for the moment, these developments may be extrapolated to the present situation. Due to the space limitation, the detailed formulas are not rewritten in this paper.

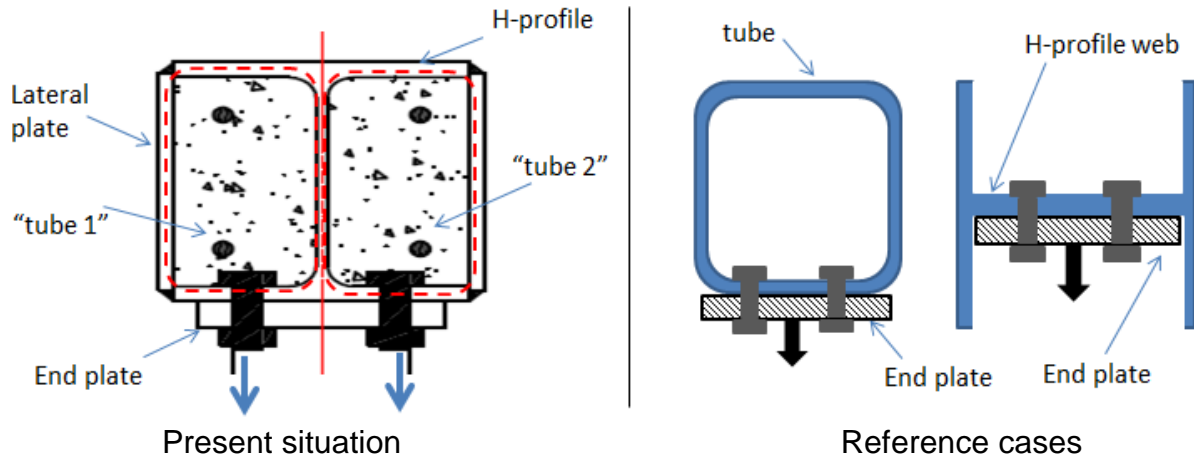


Figure 17: column flange component

3.5. Component assembly for B-EPL-RBS joint

For the determination of the joint resistance, no specific rule is needed and the method as proposed in EN1993-1-8 can be easily applied. However, for the estimation of the joint rigidity, the following method is proposed to take into account the effect of the bolt preloading.

For joints using long bolts, the preloading in the bolts has a global effect, influencing also other joint components and leading to a significant increase of the joint stiffness; the consideration of the preloading in the bolts in the determination of the joint stiffness is therefore recommended.

In the case of B-EPL-RBS joint, the bolt preloading has effects on the bolt stiffness itself but also on the stiffness of the column in transverse compression/tension component (Figure 18). Indeed, if the bolt preloading is omitted, the bolts and the column are two separate components while they work together if the preloading is considered as represented in Figure 18. The following equations can be used to estimate the effective stiffness of the “column + bolt” component in for the two cases:

$$k_{column+bolt} = (1/k_{column} + 1/k_{bolt})^{-1} \text{ (if preloading is omitted)} \quad (9)$$

$$k_{column+bolt} = k_{column} + k_{bolt} \text{ (if preloading is considered)} \quad (10)$$

where k_{column} and k_{bolt} are respectively the stiffness factors of the “column in compression/tension” component and “bolt in tension” component when they are considered in isolation, using the formulas recommended in EN1993-1.8 and EN1994-1.1.

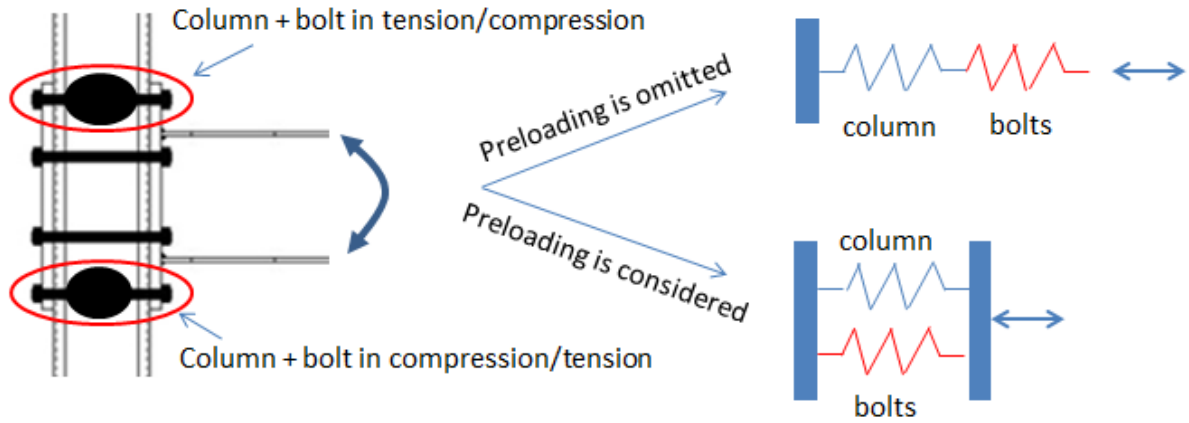


Figure 18: effect of the bolt preloading on the joint stiffness

3.6. Resistance of the beam in the hammer head zone

The resistance of the beam in the hammer head zone should be verified to avoid the development of a plastic hinge in this part.

Let consider a section of a distance s from the hammer head end (Figure 19). Two possible failure modes corresponding in two sections (1-1 and 2-2) are identified. The resistance of Section 1-1 can be easily estimated. For Section 2 combining the bending resistance of the beam and the shear resistance of the hammer head web, the resistance can be estimated as follows:

$$M_{Rd, hammer\ head\ zone} = M_{Rd, beam} + f_{yw} t_w s h_b / \sqrt{3} \quad (11)$$

where $M_{Rd, beam}$ is design resistance of the I-profile; f_{yw} is the yield strength of the hammer head web material; s is the distance represented in Figure 19; h_b is the beam height.

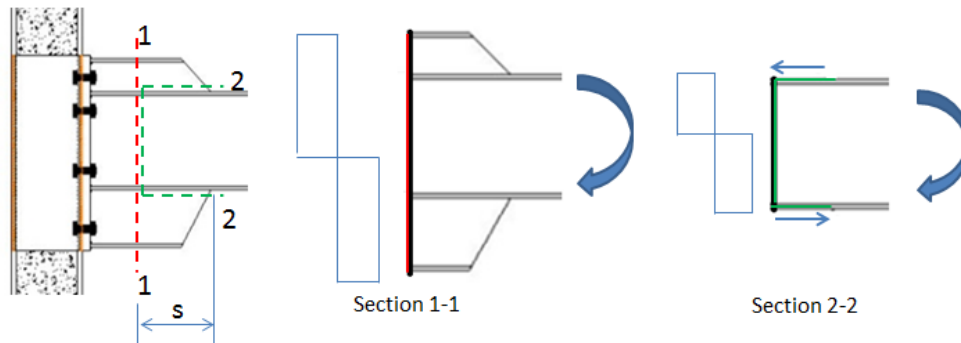


Figure 19: resistance of the beam in the hammer head zone

4. VALIDATION OF THE PROPOSED MODELS

The proposed analytical models for the joint designs provided in Section 3 are validated through comparisons to the experimental results presented in Section 2. In order to make the comparison, the actual material characteristics obtained through coupon tests are used; concerned values are given in Table 4. Moreover, all partial safety factors are taken as equal to 1,0. The organisation of the validation procedure is summarized in Table 5. Not only the final results are given but also the calculation procedures to explain the application of the proposed rules. Very good agreements are observed demonstrating the accuracy of the proposed models.

Table 4: coupon test results

Elements	Yielded strength	Ultimate strength
Bolts		606,0 kN/bolt
Beam/hammer head flange	396,0 N/mm ²	490,0 N/mm ²
Beam/hammer head web	430,0 N/mm ²	512,0 N/mm ²
U front face (C specimens)	448,5 N/mm ²	538,5 N/mm ²
U lateral faces (C specimens)	420,5 N/mm ²	526,0 N/mm ²
U lateral and front face (E specimens)	440,0 N/mm ²	530,0 N/mm ²
Using the actual strengths, the plastic and ultimate capacities of the IPE400 beam are respectively: $M_{yield,beam} = 500,0$ kNm; $M_{ultimate,beam} = 613,3$ kNm		

Table 5: validation of the proposed models

Proposed models to be validated	Reference tests	Details
Assembly procedure to calculate the bending resistance of B-EP-H joint	A2 and B1	Table 6 Table 7
U channel component capacity	C1, C2, E1 and E2	Table 8
Resistance of beam in the hammer head zone	A1	Table 9
Account for the preloading in the calculation of the stiffness for the B-EPL-RBS joints	D1, D2, F1 and F2	Table 10 Table 11

Table 6: ultimate strength of B-EP-H joint under hogging moment

Critical components and resistances (kN)	Compression forces (kN)
Row 1: bolt in tension, $F_{Rd,row1}=1212$ (Table 4)	$F_{zone1}=1175$ (Eq.(1)) $F_{zone2}=1249$ (Eq.(2))
Row 2: bolts in tension, $F_{Rd,row2}=1212$ (Table 4)	
Zone 1: hammer head in shear, $F_{Rd,zone1}=1175$ (Eq.(3))	
Zone 2: beam flange and web in compression, $F_{Rd,zone2}=1295$	
Lever arms (m): $z_{11}=0,688$; $z_{12}=0,453$; $z_{21}=0,551$; $z_{22}=0,316$ (Figure 13)	
Bending resistance of joint (model): $F_{zone1}z_{11} + (F_{Rd,row1} - F_{zone1})z_{12} + F_{Rd,row2}z_{22} = 1208$ kNm	
Bending resistance of joint (B1 test):	1160 kNm
Model-test difference:	4,1%

Table 7: Ultimate strength of B-EP-H joint under sagging moment

Critical components and resistances (kN)	Compression forces (kN)
Row 1: bolt in tension, $F_{Rd,row1}=1212$ (Table 4)	$F_{zone1}=1175$ (Eq.(1)) $F_{zone2}=1249$ (Eq.(2))
Row 2: bolts in tension, $F_{Rd,row2}=1212$ (Table 4)	
Zone 1: hammer head in shear, $F_{Rd,zone1}=1175$ (Eq.(3))	
Zone 2: beam flange and web in compression, $F_{Rd,zone2}=1295$	
Lever arms (m): $z_{11}=0,688$; $z_{12}=0,553$; $z_{21}=0,451$; $z_{22}=0,316$ (Figure 13)	
Bending resistance of joint (model): $F_{zone1}z_{11} + (F_{Rd,row1} - F_{zone1})z_{12} + F_{Rd,row2}z_{22} = 1212$ kNm	
Bending resistance of joint (A2 test):	1187 kNm
Model-test difference:	2,1%

Table 8: Yielding load of B-EP-U joint

Quantities (units: kN and m)	specimens			
	C1	C2	E1	E2
$F_{U,row1}$ (Eq.(4))	690,9	690,9	640,7	640,7
$F_{U,row2}$ (Eq.(5))	273,3	472,9	301,4	521,4
$F_{U,zon1}$ (Eq.(6))	820,0	730,0	942,1	1162,1
$F_{U,zon2}$ (Eq.(7))	144,2	433,8	0,0	0,0
Yielding moment (model)	587,6	630,0	606,87	675,9
Yielding load (model)	250,0	268,0	255	284,0
Yielding load (tests)	267,0	256,0	293	287,0
Model-test differences	6,4%	4,7%	12,9%	1,0%

Note: the “test” values of the yielding moment are dervied from the bi-linear characterisation of the load-displacement cuvres with 15% of the initial stiffness assumed for the post-elastic behaviour (Figure 20), see Mágala-Chuquitaype (2010a).

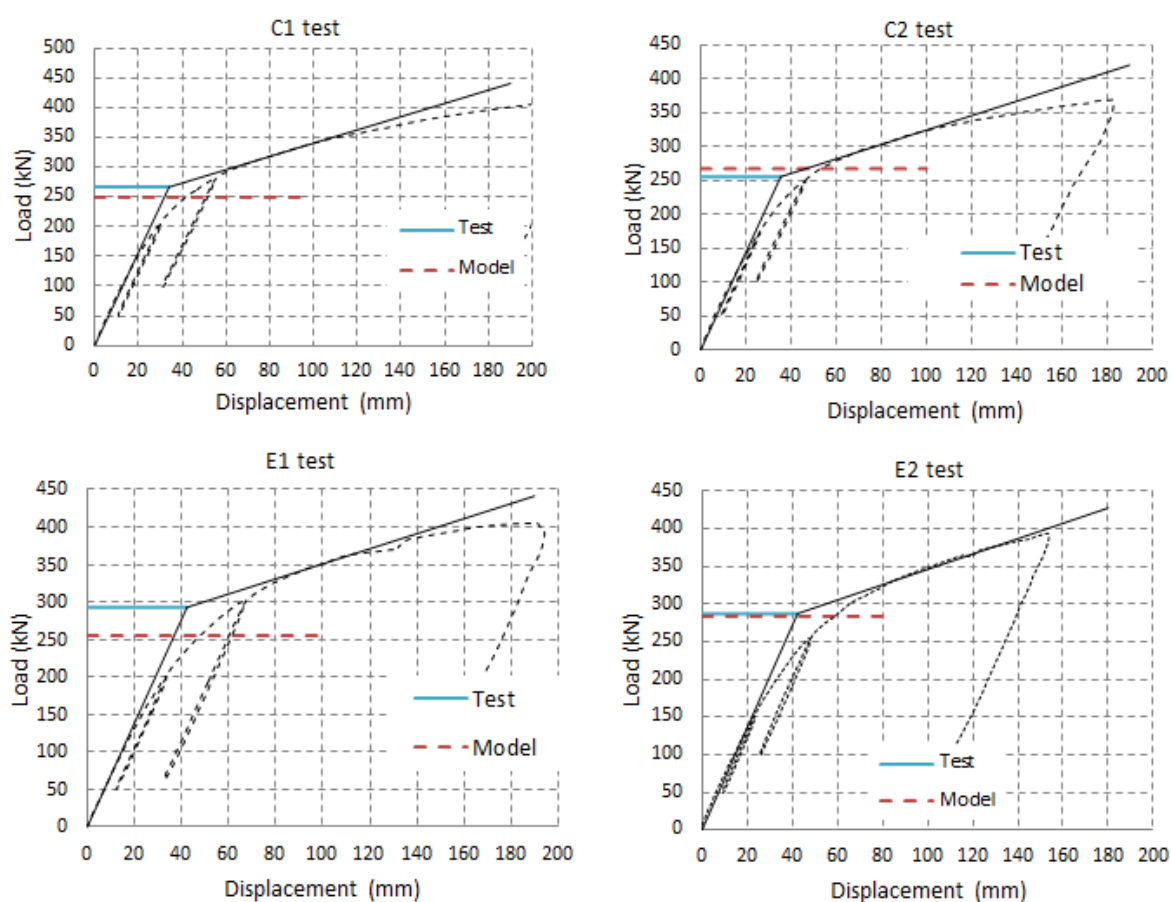


Figure 20: test vs.model comparison of the yielding loads

Table 9: bending resistance of the beam in the hammer head zone

Section position(Figure 19)	s=0,2 (A1 specimen)
IPE400 ultimate capacity (kNm)	613,3 (Table 4)
Hammer head contribution (kNm)	203,7 (Eq.(11))
Total (“section 2-2” resistance) (kNm)	817,0
Maximal bending of the A1 test	820,0 (Table 2)
Model-test difference	0,36%

Table 10: B-EPL-RBS joint - stiffness factors for the components (Comeliau (2012a))

Component	Stiffness factors (mm)	
	D configuration	F configuration
Column panel in shear ($\beta=1$)	$k_1= 9,285$	$k_1= 6,311$
Column in transverse compression (joint side)	$k_2= 22,876$	$k_2= 20,789$
Column in transverse compression (opposite side)	$k_{3,r1}= 23,028$	$k_{3,r1}= 21,331$
	$k_{3,r2}= 24,412$	$k_{3,r2}= 22,690$
End-plate in bending	$k_{4,r1}= 6,412$	$k_{4,r1}= 6,412$
	$k_{4,r2}= 52,551$	$k_{4,r2}= 89,261$
Bolts in tension	$k_{5,r1}= 2,222$	$k_{5,r1}= 2,536$
	$k_{5,r2}= 2,777$	$k_{5,r2}= 3,169$
Lever arms: $z_1=493,25$ mm; $z_2=316,25$ mm;		
Note: the components with stiffness factors equal to infinity are not reported.		

Table 11: B-EPL-RBS joint – stiffness assembly

The preloading is omitted	The preloading is considered
Effective stiffness of each bolt row (mm)	
$k_{eff,r1} = \left(\frac{1}{k_{3,r1}} + \frac{1}{k_{4,r1}} + \frac{1}{k_{5,r1}} \right)^{-1} = 1,54/1,67^{(*)}$	$k_{eff,r1} = \left(\frac{1}{k_{3,r1} + k_{5,r1}} + \frac{1}{k_{4,r1}} \right)^{-1} = 5,11/5,05$
$k_{eff,r2} = \left(\frac{1}{k_{3,r2}} + \frac{1}{k_{4,r2}} + \frac{1}{k_{5,r2}} \right)^{-1} = 2,38/2,70$	$k_{eff,r2} = \left(\frac{1}{k_{3,r2} + k_{5,r2}} + \frac{1}{k_{4,r2}} \right)^{-1} = 17,92/20,05$
Equivalent lever arm (mm)	
$z_{eq} = \frac{k_{eff,r1}z_1^2 + k_{eff,r2}z_2^2}{k_{eff,r1}z_1 + k_{eff,r2}z_2} = 405,14/403,31$	$z_{eq} = \frac{k_{eff,r1}z_1^2 + k_{eff,r2}z_2^2}{k_{eff,r1}z_1 + k_{eff,r2}z_2} = 370,77/366,17$
Equivalent stiffness factor (mm)	
$k_{eq} = \frac{k_{eff,r1}z_1 + k_{eff,r2}z_2}{z_{eq}} = 3,73/4,16$	$k_{eq} = \frac{k_{eff,r1}z_1 + k_{eff,r2}z_2}{z_{eq}} = 22,09/24,12$
Joint stiffness (models) (kNm/rad)	
$S_{J,ini} = \frac{Ez_{eq}^2}{\frac{1}{k_{eq}} + \frac{1}{k_1} + \frac{1}{k_2}} = 82986 / 77383$	$S_{J,ini} = \frac{Ez_{eq}^2}{\frac{1}{k_{eq}} + \frac{1}{k_1} + \frac{1}{k_2 + k_{5,r1}}} = 149720 / 115970$
Test stiffness (kNm/rad)	
149967 / 113539	
Model-test differences	
45% / 32%	0,16% / 2,1%
(*): ".../..." means value for the D configuration / value for the F configuration	

5. CONCLUSIONS

Within the present paper, three innovative beam-to-column joint configurations for moment resisting building frames are proposed. A test campaign on 16 full-scale specimens was performed, demonstrating the appropriate behaviours of the proposed joint solutions. New analytical design rules for specific joint components, i.e. not yet covered in the design codes, have been developed and validated through comparisons to experimental results. Using the so-developed analytical models for these specific components, the proposed joint configurations

can be fully characterized (in terms of resistant bending moment and stiffness) using the component method as recommended in the Eurocodes.

REFERENCES

- Comeliau L., Demonceau J.F., Jaspart J.P (2012a). "Computation note on the design on bolted beam-to-column joints within HSS-SERF project", internal report, University of Liege.
- Comeliau L., Demonceau J.F., Jaspart J.P (2012b). "Innovative bolted beam-to-column joints for seismic resistant building frames", in Dubina, Dan; Grecea, Daniel (Eds.) Connection VII proceedings.
- EN1993-1-8-2005. European Committee for Standardization – CEN. Eurocode 3: Design of steel structures. Part 1.8: Design of joints, Brussels.
- EN1994-1-1-2005. European Committee for Standardization – CEN. Eurocode 4: Design of composite steel and concrete structures. Part 1.1: General rules and rules for buildings.
- Jaspart J.P. Pietrapertosa C., Weynand K., Busse E., Klinkhammer R (2005). Development of a full consistent design approach for bolted and welded joints in building frames and trusses between steel members made of hollow and/or open sections: application of the component method. Volume 1: practical guidelines. CIDECT Report 5BP – 4/05.
- Lui Y. Mágala-Chuquitaype C, Elghazouli A.Y. (2012) "Response and component characterisation of semi-rigid connections to tubular columns under axial load" Engineering Structures Vol. 41, (pp. 510-532).
- Mágala-Chuquitaype C., Elghazouli A.Y. (2010a) "Behaviour of combined channel/angle connections to tubular columns under monotonic and cyclic loading" Engineering Structures Vol. 32, (pp. 1600-1616).
- Mágala-Chuquitaype C., Elghazouli A.Y. (2010b) "Component-based mechanical models for blind-bolted angle connections" Engineering Structures Vol. 32, (pp. 3048-3067).